Preparation and Properties of Microporous Cellulose Membranes from Novel Cellulose/Aqueous Sodium Hydroxide Solutions

Yu Cao,[1] Huimin Tan[2]

[1]*State Key Laboratory of Polymer Physics and Chemistry, Institute of Chemistry, Chinese Academy of Sciences, Beijing 100080, People's Republic China*
[2]*School of Materials Science, Beijing Institute of Technology, 5 South Zhongguancun Street, Beijing, 100081, People's Republic China*

Received 6 August 2005; accepted 11 December 2005
DOI 10.1002/app.23937
Published online in Wiley InterScience (www.interscience.wiley.com).

ABSTRACT: Microporous cellulose membranes were prepared from novel cellulose/aqueous sodium hydroxide solutions by coagulation with aqueous H_2SO_4 solutions. The free and glass-contacting surface morphology of the microporous cellulose membranes showed an asymmetric porous structure. The morphological structure, tensile properties, and permeability of the microporous cellulose membranes could be controlled by changes in the coagulation conditions such as the coagulant concentration and the coagulation time. © 2006 Wiley Periodicals, Inc. J Appl Polym Sci 102: 920–926, 2006

Key words: biopolymers; FTIR; membranes; morphology; structure-property relations

INTRODUCTION

Cellulose is the most abundant and renewable biopolymer on Earth.[1] It can be a primary chemical resource of the future because it is renewable, biodegradable, biocompatible, and derivatizable. Making use of cellulose not only protects the environment from pollution but also saves limited oil resources because of its potential as a substitute for some petrochemicals.

Despite the high density of hydroxyl groups in the molecule, cellulose is not soluble either in water or in aqueous alkaline solutions.[2] This is due to the existence of intramolecular and intermolecular hydrogen bonds in solid-phase cellulose that hinder the dissolution of cellulose into a solvent. The dissolution of cellulose in a solvent can be realized only by an appropriate combination of specific modifications of the structure of cellulose and solvent, except for *N*-methyl-morpholine *N*-oxide (NMMO). These regenerated cellulose fibers and membranes are prepared by viscose and cuprammonia processes in the industry and have environmental problems of waste (sometime toxic) gases and heavy metals. To meet these environmental problems, many organic solvent systems such as dimethylformamide (DMF)/nitrogen oxide, NMMO/water, dimethyl sulfoxide/paraformaldehyde, liquid ammonia/ammonium thiocyanale/water, chloral/DMF/pyridine, and dimethylacetamide/lithium chloride systems aiming at a closed process for regenerated cellulose production have been investigated. Although an industrial spinning system has been developed with NMMO/water as a cellulose solvent, most of these systems seem to still need improvement.[3–5]

The question of the direct dissolution of cellulose in an aqueous solution of sodium hydroxide (NaOH) has remained pressing over the long history of the viscose method of production of regenerated cellulose fibers. Kamide and coworkers[6–8] already succeeded in preparing completely soluble cellulose samples with crystal forms of cellulose I in 8–10 wt % aqueous NaOH solutions at low temperatures. Alkali-soluble cellulose I was prepared by a simple physical treatment (so-called steam explosion) on spruce pulp under definite conditions. In our laboratory, the solubility of various kinds of natural cellulose with an enzymatic treatment in an aqueous NaOH solution has been studied. The decrease in the viscosity-average degree of polymerization ($\overline{DP}$) and hydrogen bonding has been confirmed to govern the solubility of cellulose in about 9 wt % aqueous NaOH. The aforementioned research group made considerable effort to clarify the nature of the novel cellulose/aqueous NaOH (alkali) solution system. The utilization of the novel cellulose/aqueous alkali solution seems not to bring

Correspondence to: Y. Cao (bdcy@yahoo.com) or H. Tan (hmtan@bit.edu.cn).

TABLE I
Characteristics of the Pulp

$\overline{DP}$	α-Cellulose (%)	Ash content (%)	Fe (ppm)	Alkali absorption velocity (mm/5 min)	Swelling capacity (%)
756	92.8	0.09	7	35 × 33	408

about any serious hazards and requires no chemical regeneration process in producing fibers, membranes, and so on.[9]

Extracellular microbial enzymes have the potential to be powerful tools for modifying cellulose.[10–12] Cellulases are the enzymes that hydrolyze the β-1,4-linkages in cellulose. A cellulosic enzyme system consists of three major components: *endo*-β-glucanase (EC 3.2.1.4), *exo*-β-glucanase (EC 3.2.1.91), and β-glucosidase (EC 3.2.1.21). To date, many studies on the action of cellulases or purified cellulases on cellulose have revealed that the enzymes degrade cellulose.[12,13]

The aim of this study was to prepare regenerated cellulose membranes from cellulose in an aqueous NaOH solution with an aqueous H_2SO_4 solution as the coagulant and to investigate the morphology, structure, and physical properties of the regenerated cellulose membranes.

EXPERIMENTAL

Materials

An alkali-soluble cellulose sample ($\overline{DP}$ = 408, solubility = 100%) was prepared by the application of an enzymatic treatment to a softwood dissolving pulp (Alicell-Super Western Pulp, Ltd., Vancouver, Canada). The characteristics of the pulp are shown in Table I. Before the enzymatic treatments, the materials were disintegrated in an apparatus at the respective consistency and agitated at 3000 rpm for about 1 h.

The enzymatic treatments were incubated at 50°C under continuous agitation at 175 rpm at a 3% pulp consistency in a 50 m*M* phosphate buffer (pH 7.0) for 12 h. The enzyme concentration in the pulp treatments was based on the mass of oven-dried pulp. The dosage for the cellulase was 2 mg/g (dw)of pulp. The enzyme reactions were terminated by 15 min of boiling.

Multicomponent cellulase was derived from *Humicola insolens*. The endoglucanase (CMCase), xylanase, and filter-paper activities were measured on carboxymethylcellulose (1% carboxymethylcellulose; Sigma, St. Louis, MO), xylan (1% birchwood xylan; Sigma), and filter paper (no. 1, Whatman, Brentford, Middlesex, UK), respectively, with methods described previously. The amount of reducing sugar release was estimated by the dinitrosalicylic acid method with glucose as the standard.[14] The specific activities of cellulase are presented in Table II.

TABLE II
Specific Activities of Cellulase

Enzyme	CMCase (IU/mg)	Xylanase (IU/mg)	Filter paper (IU/mg)
Cellulase	2.07	63.2	0.21

Membrane preparation

Preparation of the cellulose/NaOH aqueous solutions

Ten grams of an alkali-soluble cellulose sample was dissolved under general stirring (500 rpm) in a 9 wt % aqueous NaOH solution at −5°C for about 8 h.[15] The resulting solution was centrifuged at 9000*G* for 30 min at 4°C to exclude the small indissoluble part and to carry out the degasification. The cellulose solution (c_a = 4.8 wt %) was used immediately to prepare regenerated cellulose membranes.

Preparation of the regenerated cellulose membranes

The cellulose solution was cast onto a glass plate (diameter = 10 cm) to give a thickness of 0.5 mm, and the glass plate was immediately immersed in coagulants. The coagulants were aqueous H_2SO_4 solutions with various H_2SO_4 concentration (c_{H2SO4}) values ranging from 2 to 20 wt % at 10°C. The coagulated membranes were washed with water for a sufficient time and then lyophilized. The membranes obtained from a 40 wt % aqueous H_2SO_4 solution were friable because of the strong dissolving action of the coagulant.

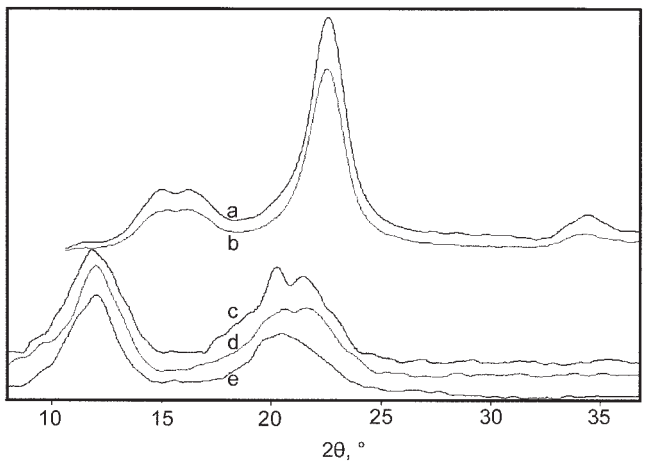

Figure 1 X-ray diffraction patterns of (a) the alkali-soluble cellulose sample, (b) the softwood pulp, and (c–e) the membranes [c_{H2SO4} = (c) 20, (d) 5, and (e) 2%].

TABLE III
X_c and ACS Values of the Membranes, Alkali-Soluble Cellulose, and Softwood Pulp

	Sample				
			Membrane		
	Softwood pulp	Alkali-soluble cellulose	2%[a]	5%[a]	20%[a]
$\overline{DP}$	756	408	369	366	367
X_c (%)	70.7 ± 1.2	81.4 ± 1.0	40.6 ± 1.1	42.1 ± 1.1	45.7 ± 1.0
ACS (nm)	5.02	6.68	4.12	4.47	4.71

[a] c_{H2SO4}.

Membrane characterization

Analyses of the pulp

The viscosity and characteristics of the pulp were measured according to the related methods of ISO/TC6 (5351/1, 1762, and 535). The carbohydrate composition of the samples was analyzed with high-performance liquid chromatography after acid hydrolysis.[16]

Determination of $\overline{DP}$

The degrees of polymerization were measured viscosimetrically in a copper ethylenediamine (CuEn) solution, and the obtained intrinsic viscosities were converted into the respective values of $\overline{DP}$ with the following equation:[17]

$$\overline{DP}^{0.905} = 0.75[\eta]_{CuEn}\ (cm^3/g)$$

where $[\eta]_{CuEn}$ is the intrinsic viscosity of CuEn.

Scanning electron microscopy (SEM) analysis

SEM analysis was performed with a Hitachi S-570 scanning electron microscope (Tokyo, Japan) operated at 25 kV. The samples were coated with gold with an Eiko IB-3 incoater (Tokyo, Japan).

Determination of the degree of crystallinity of cellulose

The molecular organization of the cellulose component, which was obtained with both control and enzymatic treatments, was measured by X-ray diffraction. After freeze drying, two slices of pulp were prepared via pressing from every sample and tested for reproducibility. The samples were scanned and recorded with a Rigaku D/max-2400 X-ray diffractometer (Rigaku, Japan) with a D-5000 rotating-anode X-ray generator at scattering angles (2θ) ranging from 10 to 40°, with Cu Kα radiation generated at 30 mA and 40 kV.

The crystallinity index (X_c) values of the cellulose samples were calculated from the X-ray diffraction patterns with the following equation:[18]

$$X_c = (I_{002} - I_{am})/I_{002} \times 100\%$$

where I_{002} is the peak intensity from the (002) lattice plane ($2\theta = 22.6°$) and I_{am} is the peak intensity of the amorphous phases ($2\theta = 19.0°$).

The apparent crystallite size (ACS) was estimated through the use of the Scherrer equation:[19]

$$ACS = 0.89 \times \lambda/\beta \cos \theta$$

where λ is the wavelength of the incident X-ray (1.5418 Å), θ is the Bragg angle corresponding to the (002)

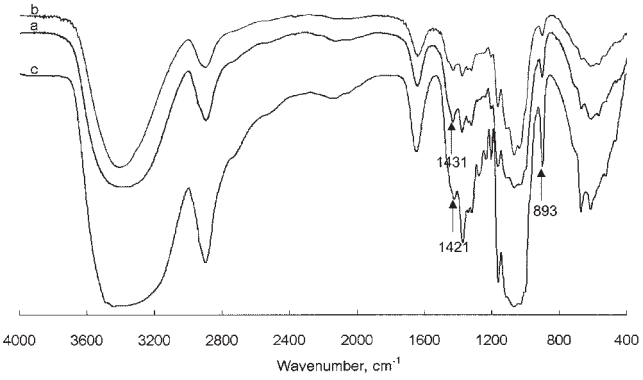

Figure 2 FTIR spectra of (a) the alkali-soluble cellulose, (b) the softwood pulp, and (c) the membranes.

TABLE IV
Intensity Ratios ($R = A_{896}/A_{1429}$) of the Samples

	Sample		
	Membranes	Alkali-soluble cellulose	Softwood pulp
R	0.74	0.40	0.46

A896, FTIR absorbance in 896 cm^{-1}; A1429, FTIR absorbance in 1429 cm^{-1}.

TABLE V
Carbohydrate Composition (Dry Weight Percentage) of the Samples

Sample	Glucose	Xylose	Mannose
Original	93.2	3.9	2.9
Membrane	92.5	4.3	3.2

plane, and β is the half-height width of the peak angle of the 002 reflection.

Fourier transform infrared (FTIR) spectroscopy

FTIR spectra were obtained with a PerkinElmer 2000 FTIR system spectrometer. The scanned wave-number range was 4000–350 cm^{-1}. After being milled, the powder of the samples was compacted into KBr disks and analyzed.

Tensile properties

The tensile properties of the porous membranes were measured according to the related methods of ISO 6239-1986 with the Instron 1121 test at a strain rate of 5 mm/min at 20°C. For reproducibility, five specimens were tested from every type of membrane, and three membrane slices were prepared from every specimen and measured. Some characteristic parameters were calculated.

Water flux and permeability

The average pore radius (r) was investigated by the filtration velocity method. The ultrafiltration flux of the wet membrane was measured in a limited time under 0.1 MPa of pressure. r was calculated according to the following revised form of the Hagen–Poiseuille equation:[20]

$$r = \left(\frac{k\eta LQ}{SP_r\Delta Pt}\right)^{1/2}$$

$$k = 3.1 \times (1 - P_r^2)^{1/2}$$

$$P_r = 1 - \frac{W}{\rho\pi R^2 L}$$

where η is the absolute viscosity of the fluid, L is the thickness of the wet membrane, Q is the flux through the membrane, ΔP is the pressure difference, S is the effective area of the membrane, P_r is the porosity, k is the apparent dimension of the pore distribution, t is the time of measurement, W is the weight of the dry membrane, R is the radius of the wet membrane, and ρ is the polymer density.

The water permeability (J) for the wet membrane was measured on miniature ultrafiltration equipment under 0.1 MPa of pressure at 20°C with the following equation:

$$J = \frac{Q}{tS}$$

RESULTS AND DISCUSSION

Structure of the membranes

Figure 1 shows the X-ray diffraction patterns of the regenerated cellulose membranes, the alkali-soluble cellulose sample, and the softwood pulp. The crystalline form of cellulose I has typical diffraction peaks at 2θ values of 14.7, 16.3, and 22.5°.[21] Cellulose with an enzymatic treatment is crystallographically cellulose I.[22] The separation of the two peaks observed at 2θ values of 14.7 and 16.3° [$(10\bar{1})$ plane] becomes better for cellulose with enzymatic treatments. The peak for the (002) plane (2θ = 22.5°) in the intensity profiles of the treated cellulose becomes sharper than that of the original samples. Peaks at 2θ values of 12, 20, and 22° in the regenerated cellulose membranes correspond to the $(1\bar{1}0)$, (110), and (200) planes, respectively, indicating a typical cellulose II crystalline form.[21]

The X_c and ACS values of the samples are listed in Table III. The increase in the X_c and ACS values of cellulose is good evidence that the amorphous portion of the cellulose is more readily and quickly hydrolyzed than the crystalline portion. X_c of the regenerated cellulose membranes ranges from 40.6 to 45.7%; these values are lower than those of the alkali-soluble cellulose sample and the softwood pulp. X_c of the membranes increases significantly with an increase in c_{H2SO4}. The enhancement of c_{H2SO4} accelerates the cellulose coagulation, so the number and development speed of the crystal improve.

The peak intensities of the (110) and (200) planes and the ACS values of the membranes increase significantly with an increase in c_{H2SO4} up to 15 wt %, but the ACS values then decrease as c_{H2SO4} increases further up to 30 wt %. The $(1\bar{1}0)$ plane experiences little change in the membranes obtained from different coagulation concentrations. The results show that the cellulose molecules coagulating from the cellulose/aqueous NaOH solutions develop crystalline packing first on the $(1\bar{1}0)$ plane and then on the (110) and (200) planes.

All the FTIR spectroscopy data are shown in Figure 2. The FTIR spectra of the regenerated cellulose membranes exhibit the characteristic absorption of cellulose II. The band near 1430 cm^{-1} is representative of the CH_2 scissoring motion.[21] The band at 1422 cm^{-1} for the cellulose membranes is weakened and shifted to a low wave number in comparison with the peak

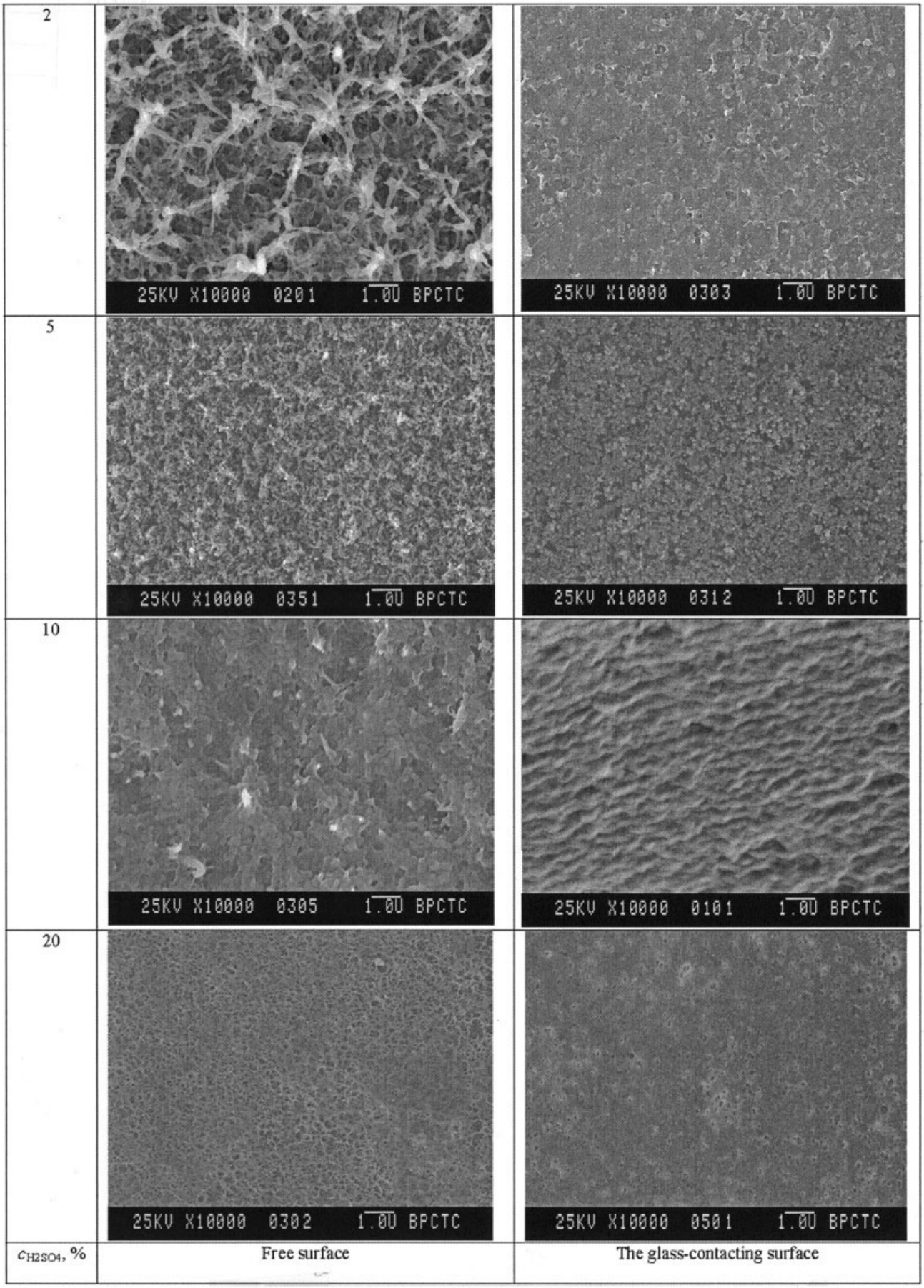

Figure 3 SEM photographs of the membranes with various c_{H2SO4} values.

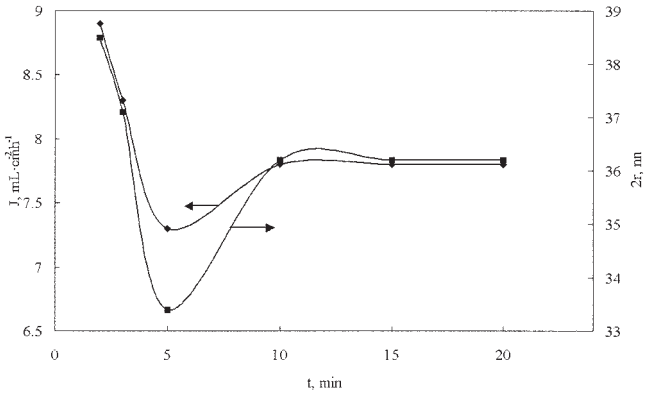

Figure 4 (■) $2r$ (nm) and (♦) J (mL·cm^{-2}·h^{-1}) of the membranes at various coagulation times.

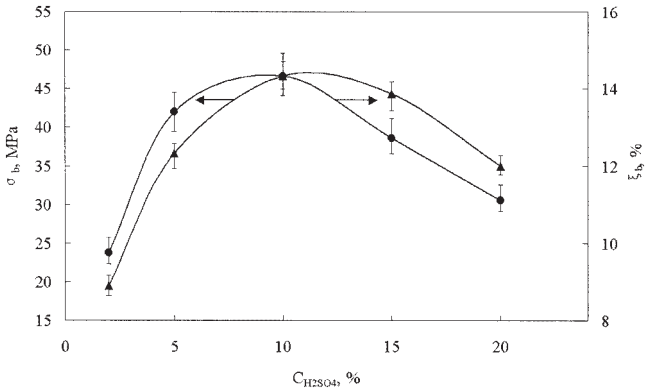

Figure 5 (▲) Tensile strength (σ_b; MPa) and (●) breaking elongation (ξ_b; %) of the membranes with various values of c_{H2SO4} (the cellulose solution was coagulated at 5°C for 10 min).

for the cellulose. This indicates the destruction of an intramolecular hydrogen bond involving the exocyclic primary hydroxyl groups (O_6). The band at 1429 cm^{-1} characterizes the crystalline state of cellulose, and the band at 893 cm^{-1} characterizes the amorphous regions of cellulose.[21] In comparison with the alkali-soluble cellulose and the softwood pulp, the bands at 1429 and 896 cm^{-1} for the membrane become weaker and stronger in Table IV. This suggests that the crystallinity of the membranes is lower than that of the alkali-soluble cellulose sample and the softwood pulp.

This shows that there are not obvious differences in the carbohydrate compositions of the original sample and dissolved parts of the samples from Table V and the FTIR spectroscopy data.

The FTIR spectroscopy data and X-ray diffraction results show that a transition from cellulose I to cellulose II takes place in the membrane formation process.

Membrane morphology

Figure 3 shows SEM pictures of the free surface (the side directly in contact with the coagulant) and fracture surface (the glass-contacting side) of the membranes. All the membranes have an asymmetric structure; that is, the pore size on the free surface is larger than that on the coagulant-contacting surface. The membranes, which were obtained from aqueous H_2SO_4 solutions with c_{H2SO4} values of 2, 5, and 10 wt %, display a homogeneous porous structure and have a network pattern on the surface. When c_{H2SO4} increases up to 20 wt %, the coagulated membranes exhibit a porous structure on the surface. The membrane morphology strongly depends on the rate of mass exchange during the coagulation process. The penetration rate of the coagulation solution on the coagulant-contacting side is faster than that on the glass-contacting side. In this result, the membrane has an asymmetric structure. The porous structure of the membrane can be controlled by changes in the coagulant composition. The membrane morphology is controlled by the interrelationship of the penetration rate of the coagulation solution and the leak-out rate of the solvent. Therefore, the preparation conditions of the membrane, such as the composition of the solvent, the polymer concentration, and the coagulation condition, are very important factors determining the membrane structure when the membrane is prepared.

Water flux and pore size of the membranes

Figures 4 shows the dependence of the mean pore diameter ($2r$) and J of the membranes on the coagulation time. Table VI shows the dependence of P_r, $2r$, and J of the membranes on the coagulation condition.

TABLE VI
Dependence of P_r, $2r$, and J of the Membranes Under the Coagulation Condition

c_{H2SO4} (%)[a]	J (mL cm^{-2}·h^{-1})	P_r (%)	$2r$ (nm)	Temperature (°C)[b]	J (mL cm^{-2} h^{-1})	P_r (%)	$2r$ (nm)
2	7.20	83.7	32.4	0	7.45	84.6	35.7
5	7.21	84.2	32.4	5	7.80	85.1	36.2
10	7.80	85.1	36.2	10	8.31	85.4	37.4
20	8.37	85.3	37.8	15	9.69	86.0	39.5

[a]The cellulose solution (c_a = 4.8 wt %) was coagulated at 5°C for 10 min. [b]The cellulose solution (c_a = 4.8 wt %) was coagulated with a 10 wt % H_2SO_4 aqueous solution for 10 min.

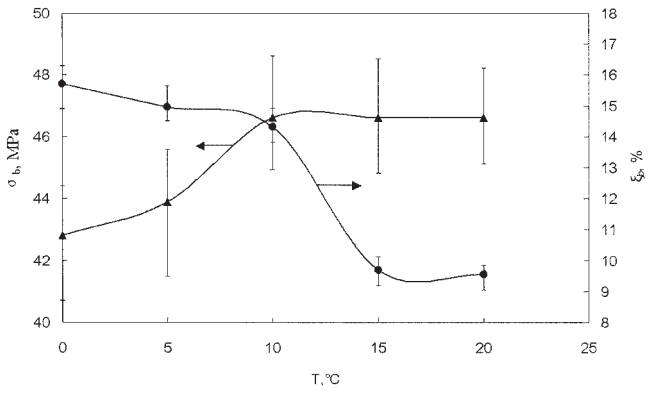

Figure 6 (▲) Tensile strength (σ_b; MPa) and (●) breaking elongation (ξ_b; %) of the membranes at various coagulation temperatures (the cellulose solution was coagulated with a 10 wt % H_2SO_4 aqueous solution for 10 min).

P_r of the membranes hardly changes with the coagulation condition and lies in the range of 83.7–86%. The $2r$ and J values of the membranes increase with increasing coagulant concentration and decrease sharply with an increase in the coagulant time to achieve the minimum value for 5 min and then increase. The changing tendency of $2r$ of the membranes with the coagulation time and coagulant concentration is similar to that of the coagulant-contacting surface. Therefore, changing the coagulation condition can adjust the pore size and permeability of the cellulose membranes.

In the asymmetric membrane, the structure of the skin layer on the coagulant-contacting side or its pore size is usually attributed to molecular-sieving characteristics in ultrafiltration. Furthermore, the membrane permeation properties are caused by the interplay of the membrane structure and the hydrophobicity/hydrophilicity of the surface.

Tensile performances of the membranes

The tensile properties are shown in Figures 5 and 6. The tensile strength and breaking elongation of the membranes in the dry state are changed by the coagulation condition, as shown in Figure 5. With the coagulation concentration increasing, the membrane structure becomes more compact, as observed in the SEM pictures, and the tensile properties of the membranes improve. The tensile properties of the membranes increase with an increase in c_{H2SO4} and achieve the values of 46.62 MPa and 14.32%, respectively, when the coagulation concentration is 10 wt %. A much higher value of c_{H2SO4} results in the reduction of the tensile properties of the membranes. The dependence of the tensile properties of the membranes on the coagulation temperature is shown in Figure 6. The tensile strength of the membranes increases at first and then achieves steady values when the coagulation temperature is over 10°C. There is a much smaller drop in the beginning of the curve of the breaking elongation of the membranes, and then it decreases suddenly when the coagulation time is over 10°C. The membrane from coagulation with 10 wt % H_2SO_4 at 10°C displays good tensile properties. Moreover, the tensile properties can be controlled by the coagulation condition.

CONCLUSIONS

Microporous cellulose membranes were prepared satisfactorily from novel cellulose/aqueous NaOH solutions by coagulation with aqueous H_2SO_4 solutions. The microporous cellulose membranes had the cellulose II crystalline form and X_c values of 40.6–45.7%, which are lower than those of an alkali-soluble cellulose sample and softwood pulp. The free surface and glass-contacting surface of the microporous cellulose membranes showed an asymmetric porous structure. The morphological structure, tensile properties, and permeability of the microporous cellulose membranes could be controlled by changes in the coagulation conditions, such as the coagulant concentration and the coagulation time. The membrane from coagulation with 10 wt % H_2SO_4 at 10°C displayed good tensile properties.

References

1. Schurz, J. Prog Polym Sci 1999, 24, 481.
2. Jarvis, M. Nature 2003, 426, 611.
3. Rosenau, T.; Potthast, A.; Sixta, H.; Kosma, P. Prog Polym Sci 2001, 26, 1763.
4. Rosenau, T.; Hofinger, A.; Potthast, A.; Kosma, P. Polymer 2003, 44, 6153.
5. Fink, H.-P.; Weigel, P.; Purz, H. J.; Ganster, J. Prog Polym Sci 2001, 26, 1473.
6. Yamashiki, T.; Saitoh, M.; Yasuda, K.; Okajima, K.; Kamide, K. Cellul Chem Technol 1990, 24, 237.
7. Yamashiki, T.; Matsui, T.; Saitoh, M.; Okajima, K.; Kamide, K. Br Polym J 1990, 22, 121.
8. Kamide, K.; Saito, M.; Kowsaka, K. Polym J 1987, 19, 1173.
9. Falt, S.; Wagberg, L.; Vesterlind, E. L.; Larsson, P. T. Cellulose 2004, 11, 151.
10. Rabinovich, M. L.; Melnik, M. S.; Boloboba, A. V. Appl Biochem Microbiol 2002, 38, 305.
11. Schulein, M. Biochim Biophys Acta 2000, 1543, 239.
12. Bhat, M. K. Biotechnol Adv 2000, 18, 355.
13. Gan, Q.; Allen, S. J.; Taylor, G. Process Biochem 2003, 38, 1003.
14. Wood, T. M.; Bhat, G. R. Methods Enzymol 1988, 160, 87.
15. Cao, Y.; Tan, H. Carbohydr Res 2002, 337, 1453.
16. Olkkonen, C.; Tylli, H.; Forsskahl, I.; Fuhrmann, A.; Hausalo, T.; Tamminen, T.; Hortling, B.; Janson, J. Holzforschung 2000, 54, 397.
17. Brown, W.; Wikstrom, R. Eur Polym J 1965, 1, 1.
18. Rogovina, S. Z.; Zhorin, V. A.; Shashkin, D. P.; Yenikolopyan, N. S. Polym Sci USSR 1989, 31, 1376.
19. Yen, J.; Mo, Z. Modern Polymer Physics; Chinese Science: Beijing, 2001.
20. Kuhn, W.; Grenze, Z. Phys Chem 1951, 55, 207.
21. Marchessault, R. H.; Sundararajan P. R. In The Polysaccharides; Aspinal, G. O., Ed.; Academic: New York, 1983.
22. Cao, Y.; Tan, H. M. Carbohydr Res 2002, 337, 1291.